

RSC Advances



This is an *Accepted Manuscript*, which has been through the Royal Society of Chemistry peer review process and has been accepted for publication.

Accepted Manuscripts are published online shortly after acceptance, before technical editing, formatting and proof reading. Using this free service, authors can make their results available to the community, in citable form, before we publish the edited article. This *Accepted Manuscript* will be replaced by the edited, formatted and paginated article as soon as this is available.

You can find more information about *Accepted Manuscripts* in the [Information for Authors](#).

Please note that technical editing may introduce minor changes to the text and/or graphics, which may alter content. The journal's standard [Terms & Conditions](#) and the [Ethical guidelines](#) still apply. In no event shall the Royal Society of Chemistry be held responsible for any errors or omissions in this *Accepted Manuscript* or any consequences arising from the use of any information it contains.

Large grained single-crystalline-like Germanium thin film on flexible Ni-W tape

Pavel Dutta,^a Monika Rathi,^a Yao Yao,^a Ying Gao,^a Goran Majkic,^a Milko Iliev,^b James Martinez,^c Bernhard Holzapfel,^d Venkat Selvamanickam^a

^a Department of Mechanical Engineering and Texas Center for Superconductivity, University of Houston, Houston, TX 77204, USA

^b Texas Center for Superconductivity and Physics Department, University of Houston, Houston, TX 77004, USA

^c Materials Evaluation Laboratory, NASA JSC Space Center, Houston, TX 77085, USA

^d Karlsruhe Institute of Technology, Karlsruhe 76021, Germany

Abstract: Roll-to-roll processing of single-crystalline semiconductor thin films on low-cost flexible substrates is of high importance for flexible electronics and photovoltaic application. In this paper we demonstrate roll-to-roll (R2R) heteroepitaxial deposition of single-crystalline-like Ge thin film on flexible cube-textured Ni-W metal substrates using an intermediate buffer layer of CeO₂. Strongly biaxially-textured Ge thin film with large grain sizes in the range of 30 - 60 μm was obtained. The Ge film exhibited (004) out-of-plane orientation and (111) in-plane orientation spread of 6.6°. Transmission Electron Microscopy (TEM) diffraction patterns and Electron Backscattered Diffraction (EBSD) mapping confirmed the single-crystalline-like nature and highly-oriented grain structure with low angle grain boundaries. Raman measurement showed the presence of only crystalline Ge phase with TO peak width of 4.3 cm⁻¹, close to that of single-crystal Ge wafer (3.8 cm⁻¹), confirming the high crystalline quality of the film. The Ge film was p-type and exhibited high carrier mobility of ~ 690 cm²/V-s. This alternative inexpensive, flexible and lightweight single-crystalline Ge thin film template, functionally nearly equivalent to single crystal Ge, may be a potential candidate for cost-effective R2R manufacturing of optoelectronic devices.

I. Introduction

Germanium has found extensive use in various opto-electronic device applications such as in integrated circuits,^{1,2} thin film transistors,³ infra-red detectors⁴ and as a substrate for high efficiency III-V concentrator solar cells.⁵⁻⁶ Excellent structural and thermal expansion match of Ge allows epitaxial growth of high quality GaAs and related III-V materials. In addition, due to

the higher carrier mobility in Ge compared to Si, it is also a very promising candidate for high switching-speed electronic devices.^{1,7} Conventional single crystal Ge wafers have been traditionally used for most high-efficiency device applications, both as active and passive layers. But, high costs of Ge wafers and limited availability have rendered them unfeasible for large-scale commercial production of cost-effective devices. Moreover, brittleness and rigidity of Ge wafers contribute to major source of device failure during fabrication. On the other hand, thin film poly and microcrystalline Ge^{7,8} provide the advantage of low-cost fabrication but suffers from low carrier mobility and high defect density primarily due to grain boundaries. Therefore, there is a need for identifying a suitable low-cost substrate and a growth technique for epitaxial growth of single crystal-like thin film Ge with electrical properties approaching those of single crystal wafers. Ideally, if highly crystallographically textured single-crystal-like Ge thin film can be heteroepitaxially deposited on low cost flexible polycrystalline substrates with good crystal quality and high carrier mobility, it will enable cost-effective, roll-to-roll, continuous, large-scale processing of highly efficient optoelectronic devices and potentially prove to be a game-changing advancement.

Efforts have been made in the recent years to achieve device-quality crystalline Ge films having large grain size on low-cost polycrystalline and amorphous substrates. Large grain size leads to fewer grain boundaries and enhances the carrier mobility by reducing scattering and trapping of charges. Since direct growth on these substrates often leads to polycrystalline Ge with smaller grain sizes, several post-growth techniques have been used to obtain large-grained Ge structures, some of which include rapid melt growth,⁹ laser annealing,^{10,11} solid phase crystallization,¹² and metal-induced crystallization.¹³⁻¹⁴ Lower temperature processing techniques have been attempted in order to allow use of temperature-sensitive plastic substrates.¹⁵ But, most often, these techniques lead to poly-Ge with high concentration of metallic impurities resulting in poor electronic properties.

On the other end, considerable efforts have also been made to directly deposit oriented Ge on low-cost glass or polycrystalline substrates using intermediate buffered layer architectures serving as seed layer for epitaxy. Similar approaches have been investigated to grow textured Si on metal substrates as well.¹⁶⁻¹⁸ Growth of biaxially-textured Ge with (111) out of plane orientation on glass using an intermediate CaF₂ buffer layer as an epitaxy enabler was

demonstrated using ion-beam-assisted deposition (IBAD) technique.¹⁹ Single crystal-like biaxially textured Ge (111) films on glass substrates were grown using a biaxially textured CaF₂ buffer layer where the biaxial texture in CaF₂ was obtained by oblique angle deposition technique.²⁰ The grain size of Ge was reported to be ~ 50-200 nm. In another approach, biaxially textured Ge (111) with grain size 50-200 nm was obtained on rolled cube-textured Ni (200) substrates using CaF₂ (111) as an intermediate layer.²¹ The biaxial cube texture in Ni substrates was obtained by Rolling Assisted Biaxially Textured Substrates (RaBiTS) technique. In all of the studies, (111) orientation of Ge with small grain sizes instead of the technologically important (001) orientation was reported. Deposition of large grain sized (001)-oriented Ge film on flexible inexpensive substrates with properties approaching that of bulk Ge wafers has remained challenging till date.

Previously, we have successfully demonstrated continuous roll-to-roll processing of highly biaxially-textured Ge (001) thin film on flexible polycrystalline metal foils.²² The hastelloy metal foils were found to be extremely stable at elevated temperatures and this allowed epitaxial growth of Ge at 700-850°C employing multiple intermediate oxide buffer layers. Biaxially-textured MgO deposited by IBAD process on amorphous oxides on polycrystalline metal substrates provided the enabling template for epitaxial growth of single crystalline-like Ge thin films.²²⁻²³ n and p- type single crystalline-like Ge thin films with (004) out-of-plane orientation were epitaxially deposited by radio-frequency (RF) magnetron sputtering.

In this paper, we explore an alternate approach using a simpler architecture Ge/CeO₂/Ni-W for roll-to-roll growth of large-grained biaxially-textured Ge thin films on a low cost flexible substrate. In place of an IBAD template as in previous publications,^{22,23} biaxially textured Ni-W metal foil was used in this study. The texture in Ni-W was obtained by rolling-assisted biaxially textured substrates (RABiTS) approach, a well-established commercial method to develop biaxially textured metal substrates for epitaxial growth of high temperature superconductor films.²⁴ Similar to hastelloy, Ni-W tapes were also highly stable at elevated temperatures which allowed the use of high temperature regimes suitable for epitaxial growth. Since Ge does not grow epitaxially on Ni-W directly, an intermediate CeO₂ buffer layer with preferred (001) orientation was grown to provide chemical compatibility, lattice and structural match to Ge.²² All

the depositions were done in a continuous roll-to-roll (R2R) process by radio-frequency sputtering at high temperatures.

II. Experimental details

Biaxially textured $\{100\}\langle 100\rangle$ Ni-5 at.% W alloy tape, 10 mm wide and 80 μm thick, was provided by IFW Dresden. The Ni-W tapes were prepared by RABiTS approach,^{25,26} an industrially scalable thermo-mechanical process which imparts a strong biaxial texture to a metal substrate. W is known to impart added mechanical strength to the RABiTS Ni tapes and at a low content, the cube texture is preserved.²⁷ The tapes were ultrasonically cleaned in isopropyl alcohol (IPA) for 10 min and blown dry with N_2 before loading into the deposition chamber. All the depositions were done in custom-made R2R radio-frequency sputter deposition system which allowed continuous growth of films on long substrates. A schematic of the sample architecture and the R2R deposition process is shown on Fig 1(a). A photograph of flexible Ge sample is shown in the inset. The Ni-W substrates were first annealed for 10 min in Ar atmosphere at 800 C. Then, an intermediate buffer layer of CeO_2 was deposited on Ni-W in a two-step process. CeO_2 was chosen as the intermediate layer since it has a good chemical compatibility, structural and lattice match with Ge and can provide a suitable template for epitaxial Ge growth, as we have demonstrated earlier.²² In addition, a significant knowledge base was available on epitaxial growth of CeO_2 on cube textured Ni-W,²⁸⁻²⁹ commonly employed in buffer layer architecture for growth of epitaxial superconductors. In order to prevent oxidation of the Ni-W substrate, the first layer of CeO_2 was grown only in Ar atmosphere at 750°C. The chamber pressure was 5.2 mTorr and the RF power was 300 W. A 76mm diameter CeO_2 target (Plasmaterials) was used for the deposition. Next, a second layer of CeO_2 was deposited in Ar 90% + O_2 10% atmosphere at 700°C, keeping the pressure and power same as in the first step. It has been reported that O_2 promotes the growth of $(00l)$ orientation and provides texture and stoichiometry to the CeO_2 layer.³⁰ A tape speed of 1.4 cm/min was employed in both the steps. Subsequently, a Ge thin film was grown on $\text{CeO}_2/\text{Ni-W}$ in a forming gas (H_2 4% + Ar 96%) atmosphere at a temperature of 660°C, process pressure of 4.2 mTorr and RF power 250 W. A 76 mm diameter Ge target (Plasmaterials) was used during the Ge film growth. The tape speed was set at 1 cm/min and a 1.3 μm thick Ge thin film was obtained. The Ge films exhibited mirror smooth surfaces with no visible defects.

Optical images were collected using a Nikon digital microscope Model Eclipse MA200 in dark field mode. Surface morphology and roughness were analyzed using a Bruker Dimension 3000 Atomic Force Microscope. Imaging was done in tapping mode using a Si tip of 40 N/m force constant, 300 kHz frequency and 10 nm nominal tip radius. Detailed X-ray pole figure measurements were conducted using a Bruker 2D General Area Detector Diffraction System. Phi scans extracted from the pole figures were used to determine in-plane texture values. Copper $\text{k}\alpha_1$ source was used in all XRD measurements. Scanning electron microscope (SEM), model LEO 1525, was used to study the surface microstructure. Electron back scatter diffraction (EBSD) in a Supra 55VP Zeiss SEM was used to determine the local texture of the grown film. EBSD mapping was done at 20 kV in variable pressure (VP) mode to avoid sample charging using a current of 10-15 nA. Transmission electron microscope (TEM) images and diffraction patterns were obtained using a JEOL 2000FX at 200 kV operating voltage. Samples for cross sectional microstructure analysis were prepared by FEI 235 focused ion beam (FIB) milling system at an acceleration voltage of 30 kV and an ion emission current of 2 μA . Carrier mobility measurements at room temperature were performed using a custom-made Hall measurement set-up with a 1.76 T magnet. GaIn Ohmic contacts were applied to four corners of the samples and measurement was done by the Van der Pauw method. Raman spectra were measured with 458 nm (Ar^+) excitation using T64000 spectrometer equipped with a microscope with 100X objective.

III. Results and discussion

In order to determine the surface microstructure of the films, dark-field optical images of Ge/ CeO_2 /Ni-W, CeO_2 /Ni-W and Ni-W substrate were obtained. The optical image of Ge surface shown in Fig 1(b) revealed large grains varying from 30 to 60 μm with distinct grain boundaries, despite the Ge film being only $\sim 1.3 \mu\text{m}$ thick. Similar large grain sizes were observed in the CeO_2 buffer and Ni-W substrate as shown in fig 1(c) and (d) respectively. No cracks were observed in the CeO_2 buffer layer. The grain structure of the top Ge film was comparable to that of the underlying CeO_2 buffer and Ni-W substrate which suggested that the Ge grain growth followed the grain structure of the underlying layer and the large grain size of the Ni-W substrate may have promoted large grain growth of the subsequent films. Large grain size in semiconductor films grown on low-cost substrates is desirable to achieve device quality film

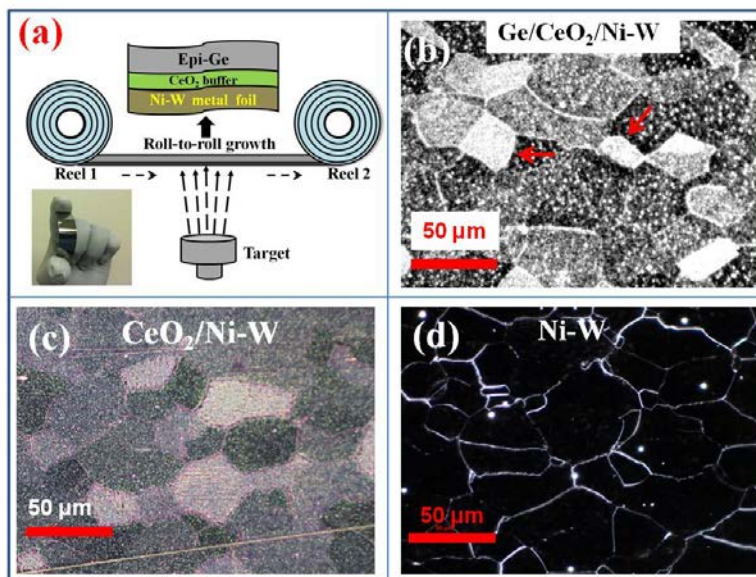


Figure 1 (a) Schematic of roll-to-roll continuous radio-frequency sputter deposition of Ge and CeO_2 on flexible Ni-W metal foils. Inset shows a photograph of R2R-grown flexible Ge sample. Optical micrographs of the surface of (b) Ge/ CeO_2 /Ni-W (c) CeO_2 /Ni-W and (d) Ni-W metal foil. Large grain sizes ($>30 \mu\text{m}$) were observed in all the samples. Few Ge grain boundaries are marked by arrows in fig (b).

since grain boundaries are known to adversely affect the electrical properties by hindering carrier transport and reducing carrier mobility by scattering and trapping. In addition, grain boundaries are preferential sites of atomic transport and electromigration-induced device failure rates are also strongly associated with grain boundaries.³¹ The grain sizes in Ge/ CeO_2 /Ni-W are 100-300 times larger than that obtained on Ge/ CaF_2 /Ni foil or on Ge/ CaF_2 /glass reported before.²⁰⁻²¹

XRD measurements were conducted to determine the crystallographic orientation and the epitaxial relationship of the CeO_2 buffer layer and Ge film. Fig 2 (a) shows a typical θ - 2θ diffraction pattern of the Ge/ CeO_2 /Ni-W film. The penetration depth of the X-ray was enough to detect reflections from underlying CeO_2 and Ni-W substrate. A single peak was observed at $2\theta = 66^\circ$ corresponding to (400) orientation of Ge which confirmed good out-of-plane texture of the Ge film. A strong (002) peak and a weaker (111) peak were observed for the CeO_2 buffer layer. The peak at $2\theta = 51.7^\circ$ with highest intensity corresponds to the (200) peak of the cube-textured Ni-W substrate. These results indicate that the CeO_2 film grown on Ni-W substrate was preferentially oriented along (002) direction. However, a fraction of misoriented (111) grains was also present in the CeO_2 film. Nevertheless, (004) out-of-plane orientation was preferred in

the Ge film grown on CeO₂ even though (111) grains were present in the CeO₂ film. One possibility may be that the texture of CeO₂ improved as the film grew thicker resulting in (001) grains predominantly near the surface of the CeO₂ and the (111) grains were primarily near the CeO₂/Ni-W interface. High density of defects, voids and crystalline misorientation at the CeO₂/Ni-W interface are indeed observed in the TEM micrographs. Therefore, the results suggest that Ge growth initiated on a (001) top surface of CeO₂ and proceeded epitaxially resulting in a textured Ge film with (400) orientation.

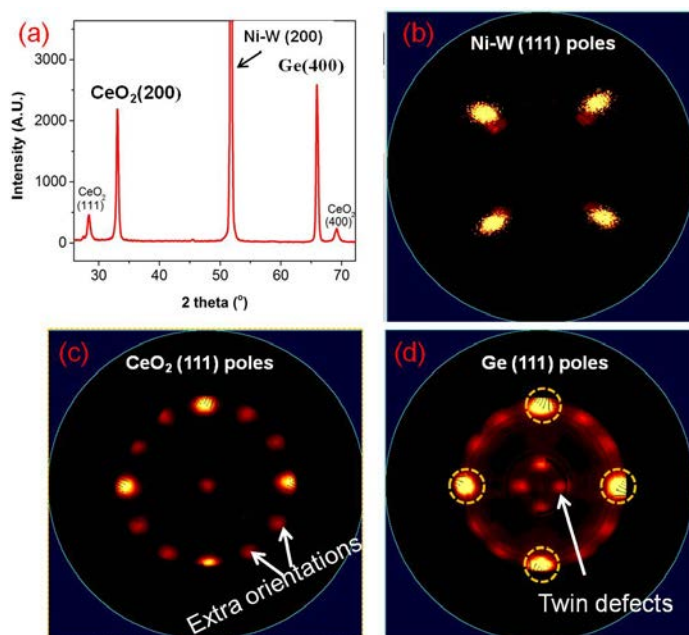


Figure 2 (a) Theta–2theta XRD patterns obtained from Ge/CeO₂/Ni-W showing strong Ge (400) peak indicating good out-of-plane texture in Ge. (111) Pole figures of (b) Ni-W substrate, (c) CeO₂ buffer and (d) top Ge showing the in-plane texture of the films. Four-fold symmetry of cube texture was observed in the films. Extra orientations in CeO₂ and reflections due to twin defects in Ge are also detected

Figure 2 (b), (c) and (d) shows the (111) pole figures of Ni-W substrate, CeO₂ layer and Ge film respectively revealing the in-plane texture of the films. A clear four-fold symmetry was observed in Ni-W indicating strong biaxial cube texture, a characteristic of RABiTS substrates. The Ni-W substrate showed a spread of ~8 degrees in the out-of-plane ~6-8 degrees in the in-plane textures. The Ni-W polefigure has a characteristic ‘spotty’ appearance, indicating many small grains scattered in orientations around the desired ‘perfect’ texture of alpha (111) = 54.74 degrees. The

scatter was present in both in-plane and out-of-plane, but was more pronounced out-of-plane. CeO₂ and Ge grew epitaxially to Ni-W as in plane: 200 (CeO₂, Ge) || 220 (Ni-W) and out of plane: 002(CeO₂, Ge) || 002 (Ni-W). This suggested that while Ni-W is textured along tape width, CeO₂ and Ge grow with (200),(020) rotated 45 degrees in plane. Since lattice constant of CeO₂ is close to $\sqrt{2}$ times Ni-W lattice constant, its epitaxial growth is expected to result in a 45° rotated alignment to realize lattice matching. The main orientations with strong intensity peaks gave rise to four-fold symmetry in CeO₂ and Ge, confirming good biaxial texture in the films. In addition, both CeO₂ and Ge exhibited two weaker in-plane orientations rotated at 30 and 60 degrees relative to the main orientation. Ge also has visible twins, as indicated in the (111) Ge pole figure, the presence of which was supported by the TEM cross-section and selected area electron diffraction patterns. In addition, CeO₂ and Ge follow the same texture as Ni-W, but their (111) peaks were smooth, characteristic of a ‘continuous’ change in orientation. The in-plane (004) and out-of plane (111) texture spread of Ge (CeO₂) were 6.5 (8) and 6.8 (6.4) degrees respectively.

Local texture investigations were performed using EBSD in order to characterize the

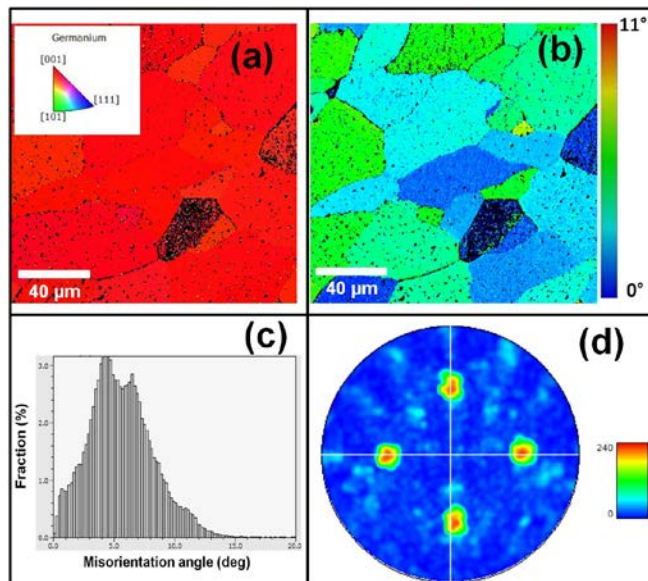


Figure 3 (a) EBSD map of Ge surface showing the preferred (001) growth of grains (b) grain and grain boundary misorientation map (c) misorientation distribution profile (d) (111) pole figure with four fold symmetry indicating biaxial texture

texture development and misorientation between the Ge grains. Fig 3 (a) shows the inverse pole figure grain orientation map along the out-of-plane direction of the film. Grains of similar orientations are given like colors. It is evident from the predominantly red color of the image that majority of the regions of the Ge film were oriented along (001) direction indicating that the film is highly textured. Only a single cubic Ge phase was identified in the EBSD maps. The high indexing rate of $\sim 98\%$ also suggested a good structural and crystalline quality of the surface. The grain boundaries, being defective, were not correctly indexed and were depicted as dark boundaries. Few grains were marked black indicating areas with non-indexed measurement due to large misorientation which may be attributed to the initial misaligned grains of the starting Ni-W substrate.³² Fig 3 (b) shows the misorientation map which also indicates that most of the regions are highly oriented with low angle grain boundaries. The misorientation distribution profile in Fig 3 (c), revealing the relative frequencies of the local angular deviation from cube orientation, shows the misorientation angle of majority of the grains and grain boundaries was below 10 degrees. The misorientation was less than 2 degrees when a much smaller region, $\sim 4 \mu\text{m}^2$ area, was mapped (not shown here), suggesting the higher crystalline quality of the Ge film on a local scale. The (111) pole figure, Fig 3 (d), also shows the four fold symmetry corresponding to the cubic texture of the Ge film and corroborates the XRD pole figure results.

Fig 4 (a) shows the TEM (220) dark field cross section image and corresponding selected area electron diffraction (SAED) patterns of the multilayer stack of Ge/CeO₂/Ni-W sample revealing the microstructure and crystallographic orientation of the individual layers. The thickness of the Ge film was found to be around 1.3 μm whereas the thickness of the CeO₂ layer was $\sim 250 \text{ nm}$. SAED pattern (Fig 4 b) acquired from the top region of the Ge film showed a diffraction pattern characteristic of diamond lattice structure, confirming successful heteroepitaxial growth on CeO₂/Ni-W. A long stacking fault propagating from the interface towards the surface along with 54.7 degree twin defects along (111) slip planes were observed in the Ge film. Appearance of extra diffractions spots in the SAED pattern (Fig 4 c) from one of the defect sites indicated the presence of the twins. High density of twins and misfit dislocations was concentrated near the Ge/CeO₂ interface which decreased towards the interior and surface of the film, leaving the top region of the Ge film relatively cleaner with fewer defects. The extended defects, such as the one shown in the image 4 (a), are also few and far between and most of the defects terminate near the interface. The reduction of defects towards the surface with increasing

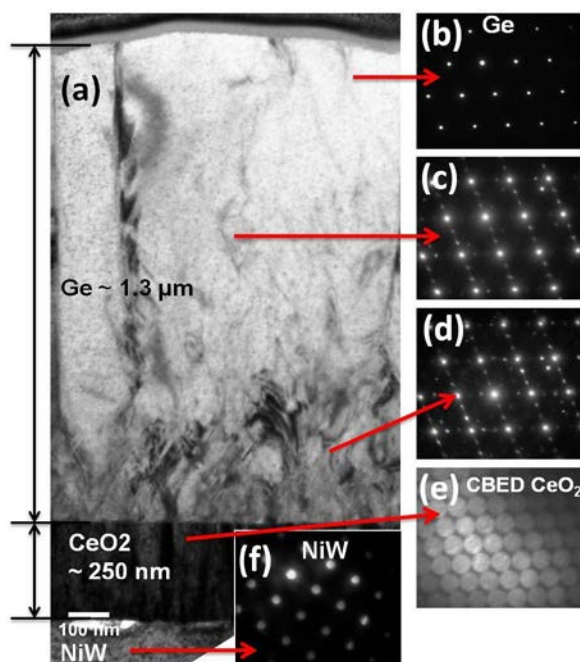


Figure 4 (a) Dark field cross-sectional TEM image of Ge/CeO₂/Ni-W showing the bulk and interfaces of the layers. SAED patterns from the (b) top (c) in the vicinity of a planar defect near the center and (d) bottom part of Ge film are shown. Characteristic spotty diffraction spots indicated epitaxial Ge growth. Appearance of additional spots in (c) and particularly from (d) suggested presence of twin defects. (e) and (f) show the disc-like CBED and spotty EBSD pattern from CeO₂ and Ni-W layer respectively indicating single-crystal-like structure

thickness can be attributed to the annihilation of dislocations with the relaxation of the film.³³ SAED pattern (Fig 4 d) acquired from a region near the interface, with the electron beam overlapping Ge and CeO₂, showed the prominence of additional primary and secondary spots corresponding to the twin defects at the interface. Due to the limitation in aperture spot size resulting in a large sampling area ~ 500 nm in SAED, convergent beam electron diffraction (CBED) was used instead in order to get information from the thin CeO₂ layer only. The CBED patterns obtained from CeO₂ film (Fig 4 e) showed characteristic discs of fluorite CeO₂ structure and confirmed the epitaxial single crystalline growth of CeO₂ on Ni-W. Since the sampling volume is small (~ 20 nm), several CBED patterns were obtained from multiple locations of the CeO₂ layer and the results always indicated the presence of crystalline CeO₂ phase in the layer. SAED pattern from Ni-W substrate also confirmed the presence of only (001) oriented crystals in the cube textured Ni-W flexible metal foil.

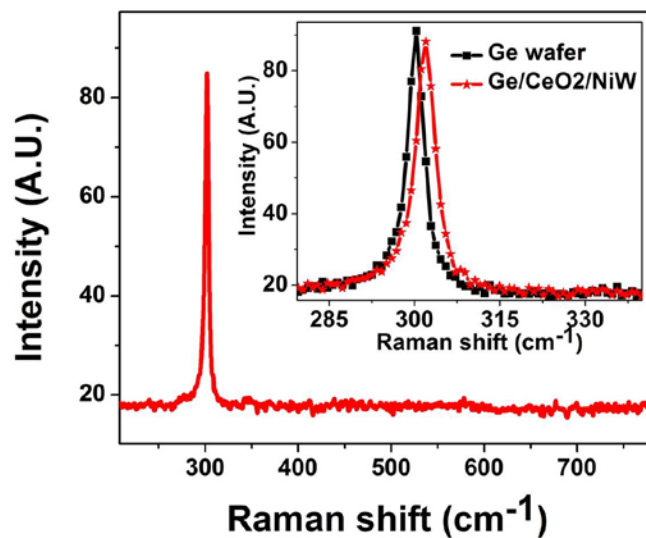


Figure 5. Raman spectrum of Ge/CeO₂/Ni-W showing the TO mode of Ge at 302 cm⁻¹ suggesting presence of only crystalline Ge phase. Inset shows the comparison of Raman spectra of Ge/CeO₂/Ni-W with that of a Ge wafer

In order to determine the crystalline quality and residual strain in the Ge film, Raman spectroscopy was utilized. The penetration depth of the 458 nm laser light used to excite the sample was estimated to be around 150 nm. Fig 5 shows the Raman spectrum of Ge/CeO₂/Ni-W sample and inset displays the magnified spectra comparing the same Ge film with a reference single crystal bulk Ge wafer. A single sharp peak of Raman transverse optical (TO) mode at 302 cm⁻¹ corresponding to crystalline Ge phase was observed.³⁴ The Ge film was purely crystalline without any amorphous phase, as indicated by the absence of the characteristic broad amorphous band at ~ 270 cm⁻¹. The inset shows the location of the Raman peak of flexible Ge film shifted slightly towards higher wavenumbers by 1.7 cm⁻¹ with respect to Ge wafer suggesting a compressively-strained Ge film. The residual strain can be attributed to the ~ 4% lattice mismatch between the Ge film and underlying CeO₂. The full-width-at-half-maximum (FWHM) of the TO peaks, a good indicator of the crystalline quality of the film, was estimated by fitting the peaks using a Lorentzian function. The presence of grains and disorder leads to broadening of the peaks due to decrease of the phonon lifetime. Therefore, a narrow peak width indicates less disorder and higher crystalline quality of a material. The Raman line FWHM value of the Ge thin film was 4.3 cm⁻¹, very close to that of the reference Ge wafer 3.8 cm⁻¹ and much narrower compared to previously reported values from thin film Ge films grown on polycrystalline substrates and silicon substrates.^{35,36}

Electrical conductivity and Hall mobility measurements were conducted at room temperature employing Van der Pauw method. The Ge film showed high electrical conductivity of $\sim 4 \times 10^6$ Siemens/cm and a carrier concentration of $3.6 \times 10^{22} \text{ cm}^{-3}$. The high carrier concentration may be attributed to thermal diffusion of Ni, W, Ce and other metallic impurities from the metal foil into the Ge film during growth at high temperatures ($>650^\circ\text{C}$). No diffusion barrier was used to limit diffusion in the present architecture and ideally, a suitable barrier layer between CeO_2 and Ni-W will be necessary to prevent undesired diffusion. The Ge thin film showed a p-type character with a high average Hall mobility of $690 \text{ cm}^2/\text{Vs}$ which may be attributed to the strong biaxial texture of the film, good crystalline quality and large grain size ($>30 \mu\text{m}$) that minimizes charge scattering at the grain boundaries. The high mobility Ge thin film may provide the ideal platform for R2R manufacturing of low-cost flexible thin film transistors, integrated circuits and related high speed electronics. Further studies are underway to achieve doping (carrier concentration) control of the Ge films by optimizing the R2R process parameters such as growth temperature, process pressure, tape speed and by using high purity Ge targets. In addition, several strategies are being investigated which include laser-induced crystallization, zone-melting recrystallization and plasma-enhanced chemical vapor deposition of Ge films in order to reduce the defect density of the Ge films on flexible Ni-W substrates.

IV. Conclusion

Roll-to-roll heteroepitaxial deposition of single-crystalline-like Ge thin film on flexible cube-textured Ni-W metal substrates using an intermediate buffer layer of CeO_2 has been demonstrated by rf sputtering. Strongly biaxially textured Ge thin film with large grain sizes in the range of $30 - 60 \mu\text{m}$ was obtained. The large grain structure of Ni-W substrate was transferred throughout the architecture. The Ge film exhibited (004) out of plane orientation and (111) in-plane spread of 6.6 degrees. The single-crystalline-like nature of Ge film was confirmed by TEM diffraction pattern and EBSD mapping. The presence of a single strong narrow Raman peak at 302 cm^{-1} (4.3 cm^{-1} FWHM) is an evidence superior crystalline quality and presence of pure crystalline phase in the Ge film. Cross-sectional TEM images showed the presence of misfit dislocations and stacking faults, particularly near the Ge/ CeO_2 interfaces, which decreased towards the top surface resulting in a relatively clean Ge surface. Hall measurement revealed a p-type Ge film with high carrier mobility of $\sim 690 \text{ cm}^2/\text{V-s}$. This inexpensive, flexible and

lightweight single-crystalline-like Ge thin film template, functionally nearly equivalent to single crystal Ge, may be a potential candidate for cost-effective R2R manufacturing of optoelectronic devices and substrates for high efficiency III-V photovoltaics.

ACKNOWLEDGEMENT

The authors would like to acknowledge Prof. Manuel Quevedo and Dr. Norberto Hernandez of the Department of Materials Science and Engineering, University of Texas, Dallas, for their help in conducting Hall mobility measurements of the samples.

REFERENCES

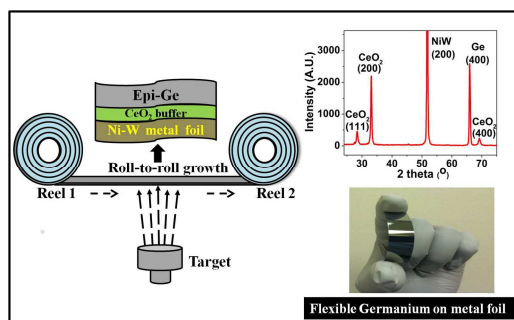
- [1] M. Bosi and G. Attolini, *Progress in Crystal Growth and Characterization of Materials*, 2010, **56**, 146-174.
- [2] H. Shang, H. Okorn-Schimdt, J. Ott, P. Kozlowski, S. Steen, E. C. Jones, H.-S. P. Wong and W. Hanesch, *IEEE Electron Device Lett.*, 2003, **24**, 242-244.
- [3] M. Miyao, E. Murakami, H. Etoh, K. Nakagawa and A. Nishida, *J. Cryst. Growth*, 1991, **111**, 912-915.
- [4] S. J. Koester, J. D. Schaub, G. Dehlinger and J. O. Chuiee, *IEEE Journal Of Selected Topics In Quantum Electronics*, 2006, **12**, 1489 – 1502.
- [5] J. Olson, S. Kurtz, A. Kibbler and A. Faine, *Appl. Phys. Lett.*, 1990, **56**, 623–625.
- [6] R. R. King, D. C. Law, K. M. Edmondson, C. M. Fetzer, G. S. Kinsey, H. Yoon, R. A. Sherif and N. H. Karam, *Appl. Phys. Lett.*, 2007, **90**, 183516.
- [7] D. Shahrjerdi, B. Hekmatshoar, S.S. Mohajerzadeh, A. Khakifirooz and M. Robertson, *Journal of Electronic Materials*, 2004, **33**, 353-357.
- [8] N. Yoshida, Y. Hatano and M. Isomura, *Sol. Energy Mater. Sol. Cells*, 2011, **95**, 175–178.
- [9] Y. Liu, M. D. Deal and J. D. Plummer. *Appl. Phys. Lett.*, 2004, **84**, 2563.
- [10] O. Salihoglu, U. Kürüm, H. G. Yaglioglu, A. Elmali and A. Aydinli, *J. Vac. Sci. Technol. B*, 2012, **30**, 011807.
- [11] C. Grigoropoulos, M. Rogers, S. H. Ko, A. Golovin and B. J. Matkowsky, *Phys. Rev. B*, 2006, **73**, 184125.

- [12] C. M. Yang and H. A. Atwater, *Appl. Phys. Lett.* 1996, **68**, 24.
- [13] F. Katsuki, K. Hanafusa, M. Yonemura, T. Koyama, and M. Doi, *J. Appl. Phys.* 2001, **89**, 4643.
- [14] J. -H Park, P. Kapur, K. C. Saraswat and H. Peng, *Appl. Phys. Lett.*, 2007, **91**, 143107.
- [15] J. -H. Park, T. Suzuki, M. Kurosawa, M. Miyao and T. Sadoh. *Appl. Phys. Lett.*, 2013, **103**, 082102.
- [16] A. T. Findikoglu, W. Choi, V. Matias, T. Holesinger, Q. Jia and D. Peterson, *Adv. Mater.*, 2005, **17**, 1527–1531.
- [17] C. W. Teplin, M. P. Paranthaman, T. R. Fanning, K. Alberi, L. Heatherly, S.-H. Wee, K. Kim, F. A. List, J. Pineau, J. Bornstein, K. Bowers, D. F. Lee, C. Cantoni, S. Hane, P. Schroeter, D. L. Young, E. Iwaniczko, K. M. Jones and H. M. Branz, *Energy Environ. Sci.*, 2011, **4**, 3346–3350
- [18] S.-H. Wee, C. Cantoni, T. R. Fanning, C. W. Teplin, D. F. Bogorin, J. Bornstein, K. Bowers, P. Schroeter, F. Hasoon, H. M. Branz, M. P. Paranthaman and A. Goyal, *Energy Environ. Sci.*, 2012, **5**, 6052-6056
- [19] J. R. Groves, J. B. Li, B. M. Clemens, V. LaSalvia, F. Hasoon, H. M. Branz and C. W. Teplin, *Energy Environ. Sci.*, 2012, **5**, 6905-6908.
- [20] C. Gaire, P. C. Clemmer, H. -F. Li, T. C. Parker, P. Snow, I. Bhat, S. Lee, G.-C. Wang and T.-M. Lu., *J. Cryst. Growth*, 2010, **312**, 607–610.
- [21] C. Gaire, J. Palazzo, I. Bhat, A. Goyal, G.-C. Wang and T.-M. Lu. *J. Cryst. Growth*, 2012, **343**, 33–37.
- [22] V. Selvamanickam, S. Sambandam, A. Sundaram, S. Lee, A. Rar, X. Xiong, A. Alemu, C. Boney and A. Freundlich, *J. Cryst. Growth*, 2009, **311**, 4553–4557.
- [23] R. Wang, S.N. Sambandam, G. Majkic, E. Galstyan and V. Selvamanickam, *Thin Solid Films*, 2013, **527**, 9–15.
- [24] D. P. Norton, A. Goyal, J. D. Budai, D. K. Christen, D. M. Kroeger, E. D. Specht, Q. He, B. Saffian, M. Paranthaman, C. E. Klabunde, D. F. Lee, B. C. Sales and F. A. List, *Science*, 1996, **274**, 755-757.
- [25] A. Goyal, D. P. Norton, J. D. Budai, M. Paranthaman, E. D. Specht, D. M. Kroeger, D. K. Christen, Q. He, B. Saffian., F. A. List, D. F. Lee, P. M. Martin, C. E. Klabunde, E. Hartfield and V. K. Sikka, *Appl. Phys. Lett.*, 1996, **69**, 1795.
- [26] V. S. Sarma, J. Eickemeyer, C. Mickel, L. Schultz and B. Holzapfel, *Mater. Sci. Eng. A*, 2004, **380**, 30–33.

- [27] J. Eickemeyer, D. Selbmann, R. Opitz, H. Wendrock, E. Maher, U. Miller and W. Prusseit, *Physica C*, 2002, **372–376**, 814–817.
- [28] X. Cui, F. A. List, D. M. Kroeger, A. Goyal, D. F. Lee, J. E. Mathis, E. D. Specht, P. M. Martin, R. Feenstra, D. T. Verebelyi, D. K. Christen and M. Paranthaman, *Physica C*, 1999, **316**, 27–33.
- [29] D. Eyidi, M. D. Croitoru, O. Eibl, R. Nemetschek and W. Prusseit, *J. Mater. Res.*, 2003, **18**, 14–26.
- [30] Q. He, D. K. Christen, J. D. Budai, E. D. Specht, D. F. Lee, A. Goyal, D. P. Norton, M. Paranthaman, F. A. List and D. M. Kroeger, *Physica C*, 1997, **275**, 155–161.
- [31] F. M. d'Heurle and I. Ames, *App. Phys. Lett.*, 1970, **16**, 80.
- [32] R. Hühne, J. Eickemeyer, V. S. Sarma, A. Güth, T. Thersleff, J. Freudenberger, O. de Haas, M. Weigand, J. H. Durrell, L. Schultz and B. Holzapfel, *Supercond. Sci. Technol.*, 2010, **23**, 1–7.
- [33] A. T. Findikoglu, W. Choi, V. Matias, T. G. Holesinger, Q. X. Jia and D. E. Peterson, *Adv. Mater.*, 2005, **17**, 1527–1531.
- [34] J. H. Parker, D. W. Feldman and M. Ashkin, *Phys. Rev.*, 1967, **155**, 712–714
- [35] G. Venugopal Rao, G. Amarendra, B. Viswanathan, S. Kanakaraju, S. Balaji, S. Mohan, and A. K. Sood, *Thin Solid Films*, 2002, **406**, 250–254.
- [36] C.-Y. Tsao, J. W. Weber, P. Campbell, P. I. Widenborg, D. Song and M. A. Green, *Appl. Surf. Sci.*, 2009, **255**, 7028–7035.

Large grained single-crystalline-like Germanium thin film on flexible Ni-W tape

Table of contents entry



Roll-to-roll growth of single-crystalline-like Germanium thin films with high carrier mobility on low-cost flexible Ni-W metal foils has been demonstrated